Early diet-induced non-alcoholic steatohepatitis in APOE2 knock-in mice and its prevention by fibrates

ELSEVIER

Journal of Hepatology 44 (2006) 732–741

Journal of Hepatology

www.elsevier.com/locate/jhep

Early diet-induced non-alcoholic steatohepatitis in APOE2 knock-in mice and its prevention by fibrates

Ronit Shiri-Sverdlov[1,7,8,†], Kristiaan Wouters[1,7,†], Patrick J. van Gorp[1,7,8], Marion J. Gijbels[1,2,7], Benoit Noel[3], Laurent Buffat[4], Bart Staels[3], Nobuyo Maeda[5], Marc van Bilsen[6,7], Marten H. Hofker[1,7,8,*]

[1]*Department of Molecular Genetics, University Maastricht, UNS40/11 P.O. Box 16, 6200 MD, Maastricht, The Netherlands*
[2]*Department of Pathology, University of Maastricht, Maastricht, The Netherlands*
[3]*U.545 Inserm, Institut Pasteur de Lille, Department d'Atherosclérose and Université de Lille2, Lille, France*
[4]*IT Omics, Lille, France*
[5]*Department of Pathology, University of North Carolina, Chapel Hill, NC, USA*
[6]*Department of Physiology, University Maastricht, Maastricht, The Netherlands*
[7]*Cardiovascular Research Institute Maastricht (CARIM), Maastricht, The Netherlands*
[8]*Nutrition and Toxicology Research Institute Maastricht (NUTRIM), Maastricht, The Netherlands*

***Background/Aims*: The molecular mechanisms leading to Non-Alcoholic Steatohepatitis (NASH) are not fully understood. In mice, NASH can be inhibited by fenofibrate, a synthetic agonist for the nuclear receptor peroxisome proliferator activated receptor alpha, which regulates hepatic triglyceride metabolism. This study aimed to elucidate the relation between steatosis and inflammation in NASH in a human-like hyperlipidemic mouse model.**

***Methods*: Liver phenotype and gene expression were assessed in APOE2 knock-in mice that were fed a western-type high fat diet with or without co-administration of fenofibrate.**

***Results*: In response to a western diet, APOE2 knock-in mice developed NASH characterized by steatosis and inflammation. Strikingly, macrophage accumulation in the liver preceded the steatosis during progression of the disease. This phenotype was in line with gene expression patterns, which showed regulation of two major groups of genes, i.e. inflammatory and lipid genes. Fenofibrate treatment decreased hepatic macrophage accumulation and abolished steatosis. Moreover, a marked reduction in the expression of inflammatory genes occurred immediately after fenofibrate treatment.**

***Conclusions*: These data indicate that inflammation might play an instrumental role during the development of NASH in this mouse model. Inhibition of NASH by fenofibrate may be due, at least in part, to its inhibitory effect on pro-inflammatory genes.**

***Keywords*: Cholesterol; Hyperlipidemia; Microarray; Non-alcoholic steatohepatitis; PPARa; Triglyceride; APOE; Steatosis; Inflammation; Western diet**

1. Introduction

Non-alcoholic steatohepatitis (NASH) is characterized by pathological alterations ranging from steatosis and inflammation to cell degeneration, fibrosis and cirrhosis [1]. The pathogenesis of NASH remains poorly understood. It is a component of the metabolic syndrome and therefore frequently associated with hyperlipidemia [2]. Indeed, several mouse models of hyperlipidemia, such as ldlr$^{-/-}$

Received 22 June 2005; received in revised form 4 October 2005; accepted 10 October 2005; available online 20 December 2005

* Corresponding author. Address: Department of Molecular, Genetics, Universiteit Maastricht, UNS40/11, P.O. Box 16, 6200 MD Maastricht, The Netherlands. Tel.: +31 43 388 1138; fax: +31 43 388 4574.
E-mail address: m.hofker@gen.unimaas.nl (M.H. Hofker).
† Both authors contributed equally to this paper.

0168-8278/$32.00 © 2005 European Association for the Study of the Liver. Published by Elsevier B.V. All rights reserved.
doi:10.1016/j.jhep.2005.10.033

and apoe$^{-/-}$ mice develop steatohepatitis upon high-fat feeding [18,19].

In order to study the development of NASH and the relationship of steatosis and inflammation, we used the 'humanized' APOE2 knock-in (APOE2KI) mouse, in which the human APOE2 allele replaces the murine apoe gene. These mice express human APOE2 under the control of the endogenous promoter sequences in a tissue specific manner and at physiological levels. APOE2 has a markedly reduced affinity for the LDL receptor, leading to a plasma lipoprotein profile resembling human type III hyperlipoproteinemia (HLP) [3].

Similar to humans, APOE2KI mice are responsive to lipid-lowering drugs such as fibrates, ligands for PPARα [3]. This nuclear receptor enhances the expression of genes involved in fatty acid (FA) uptake, esterification and β-oxidation [4] and has been shown to reverse steatohepatitis in mice [21]. Accordingly, fibrate was administrated to investigate the molecular mechanisms leading to the inhibition of NASH.

In this study, APOE2KI mice were fed a high-fat diet in the absence or presence of fenofibrate. The changes in plasma lipids, liver phenotype and gene expression were followed in time to discriminate between early (primary) and late (secondary) events related to NASH.

2. Materials and methods

2.1. Mice and diet

APOE2KI mice [3] were housed under standard conditions given free access to food and water. Experiments were performed according to Dutch laws, approved by the Committee for Animal Welfare of Maastricht University.

Ninety homozygote female mice, 13 week old, were divided into groups of 10. One group was kept on standard chow. Four groups were fed a western diet, containing 17% casein, 0.3% DL-methionine, 34% sucrose, 14.5% cornstarch, 0.2% cholesterol, 5% cellulose, 7% CM 205B, 1% vit 200, 21% butter (diet 1635, Scientific Animal Food and Engineering, Villemoisson-sur-orge, France) for 2, 4, 7 and 21 days. Four groups were put on the western-diet completed with 0.2% Fenofibrate (F6020, Sigma Aldrich, Zwijndrecht, the Netherlands) for 2, 4, 7 and 21 days. Blood samples were taken from the tail after a 4-h fast and collected in glass capillaries, coated with heparin and diethyl *p*-nitrophenyl phosphate [5] (D9286, Sigma Aldrich, Zwijndrecht, The Netherlands). Mice were sacrificed by cervical dislocation. Tissues were isolated and snap-frozen in liquid nitrogen and stored at −80 °C or fixed in 4% formaldehyde/PBS.

2.2. Plasma parameters

Total plasma cholesterol and triglyceride (TG) were measured (1489232, Cholesterol CHOD-PAP, Roche, Almere, The Netherlands; 337-B, TG GPO-trinder, Sigma Aldrich, Zwijndrecht, The Netherlands) according to manufacturer's protocols on a Benchmark 550 Micro-plate Reader (170-6750XTU, Bio-Rad, Veenendaal, The Netherlands).

Lipoprotein profiles were determined on pooled plasma samples from 10 mice using an AKTA Basic chromotography system with a Superose 6PC 3.2/30 column (Amersham Biosciences, Roosendaal, The Netherlands).

2.3. RNA isolation

Total RNA was isolated from frozen tissues homogenized in TriReagent (T9424, Sigma Aldrich, Zwijndrecht, The Netherlands) with the MiniBeadBeater (3110BXEUR, Biospec Products, Bartlesville, USA). RNA clean-up was performed using Qiagen RNeasy Mini Kit (74104, Qiagen, Venlo, The Netherlands). Quality and quantity were determined with Agilent2100 Bioanalyzer and RNA 6000 NanoLabChip (5065-4476, AgilentTechnologies, Amstelveen, the Netherlands). Applications were done according to manufacturer's protocols.

2.4. cDNA synthesis and microarray hybridization

Pools of 10 mice were made from equal amounts of RNA from each mouse. Six micrograms of pooled liver RNA was used in cDNA synthesis. Samples were hybridized to Affymetrix Mouse Expression Array 430A (900412, Affymetrix UK Ltd, High Wycombe, UK) according to manufacturer's instructions.

2.5. Microarray analysis

Raw data from the microarrays was analyzed using GeneChip Microarray Suite 5.0 (MAS 5.0, Affymetrix) and Data Mining Tools 3.1 (DMT 3.1, Affymetrix). To identify regulated genes, ANOVA analysis was applied based on probe level information with, R (http://www.r-project.org) and Bioconductor (http://www.bioconductor.org) was used. After normalization, a model was developed, based on probe level intensity for each probe set.

Genes were selected according to the *P*-value of the Diet/Treatment effect for each delay coefficient (four *P*-values per probe set) and for the multi-testing problem Bonferroni correction with a threshold of 1×10^{-6} ($\sim0.05/(22{,}000\times3)$ (number of probe set×number of test by probe set) was used. Genes with a *P*-value lower than 10^{-6} were selected.

2.6. Immunohistochemistry

Four micrometers paraffin embedded liver sections were stained with Heamatoxillin/Eosin (HE). Seven micrometers frozen-cut liver sections were fixated in acetone and stained with CD68 (FA11), Mac1 (M1/70) and Nimp1 antibodies (granulocytes) as described before [6].

2.7. Hepatic lipid analysis

Approximately, 50 mg of frozen liver tissue was homogenized for 30 s at 5000 rpm in a closed tube with 5.0 mm glass beads and 1.0 ml SET buffer (Sucrose 250 mM, EDTA 2 mM and Tris 10 mM) [7]. Complete cell destruction was done by two freeze–thaw cycles and three times passing through a 27-gauge syringe needle and a final freeze–thaw cycle. Protein content was measured with the BCA method (23225, Pierce, Rockford, IL, USA). TG were measured as described above. Protocols were done according to manufacturers instructions.

2.8. Real-time quantitative PCR

Prior to real-time quantitative PCR (QPCR), liver RNA pools of each group were reverse transcribed with the iScript cDNA synthesis kit (170-8891, Bio-Rad, Veenendaal, The Netherlands) according to manufacturers instructions. cDNA quantification was done by QPCR on an ABI Prism 7700 (Applied Biosystems, Nieuwerkerk a/d IJssel, the Netherlands) with Mastermix Plus kit for Sybr Green I (RT-SN2X-03+*, Eurogentec, Seraing, Belgium). For each gene, a standard curve was generated. Normalization was done with cyclophillin A. Specific primers sets (Table 2) were developed with Primer Express 1.5 (Applied Biosystems). Data were analyzed with SDS 1.9.1 (Applied Biosystems).

2.9. Statistical analysis

Data were analyzed using Graphpad Prism 4.0. Groups were compared using Welch-corrected 2-tailed non-paired *t*-tests. Data is expressed as means ± SEM and considered significant at $P < 0.05$.

3. Results

3.1. Effects of high-fat diet on lipid levels

Western diet, containing 21% fat and 0.2% cholesterol, induced a nearly fourfold increase in plasma cholesterol levels already after 2 days (Fig. 1A), which continued to rise to 7-fold after 21 days. Cholesterol was mainly present in VLDL and LDL, while on chow it was mainly present in HDL (Fig. 1C). TG levels (Fig. 1B) decreased as the high-fat feeding progressed, as observed previously [3]. This slight decrease was only significant after 3 weeks of high-fat feeding. Free fatty acid and glucose levels were not affected (data not shown).

3.2. Response to fenofibrate treatment

The western diet-induced rise in plasma cholesterol levels was completely abolished upon fenofibrate treatment. Cholesterol levels decreased markedly already at 2 days and were kept at basal level after 4, 7 and 21 days (Fig. 1a). Similarly, fenofibrate had a rapid lowering effect on TG (Fig. 1B). Fenofibrate-treatment induced a substantial decrease in VLDL-cholesterol. These alterations in plasma lipids levels are similar to hyperlipidemic patients treated with fibrates [8].

3.3. Liver histology

HE staining was performed to investigate the effect of the western diet in the liver. Sections showed a gradual fat accumulation in liver cells upon high-fat feeding (Fig. 2A). After 4–7 days of high-fat feeding, lipid droplets became visible (Fig. 2A, white arrows). The number and size of the droplets increased with time. Consistent with the morphological observations, biochemical analysis demonstrated a gradual increase in the hepatic content of TG while fenofibrate treatment prevented fat accumulation (Figs. 1D and 2A). Unexpectedly, already after 2 days of high-fat feeding, aggregates of inflammatory cells became visible in the HE stained-livers of the mice fed the western diet (Fig. 2A, black arrows). Immunohistochemical staining was performed to define the nature of these inflammatory cells. Compared to animals on a chow diet, already after 2 days of high-fat feeding an increase in CD68-positive cells was detectable (Fig. 2B), reflecting an increased number of Kupffer cells and macrophages. Within time, CD68-positive cells increased even further and aggregates of inflammatory cells became larger. Remarkably, fibrate treatment strongly opposed this effect (Fig. 2B).

To investigate whether the increase in CD68 marker was due to increase in the number of macrophages or proliferation of Kupffer cells, liver tissues were stained for

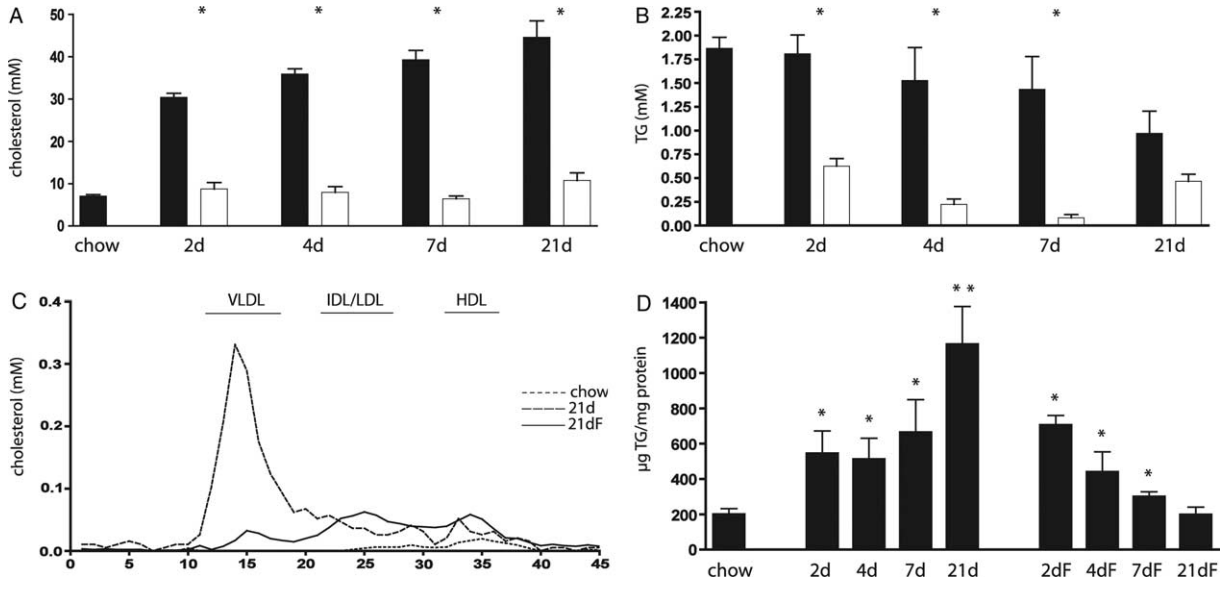

Fig. 1. Lipid parameters of the APOE2KI mice upon high-fat feeding with and without fenofibrate addition. At each time point (2 days (d), 4, 7 and 21 days), mice treated with a high-fat diet (black bars) and mice treated with a high-fat diet with fenofibrate (white bars) are shown in panels A and B. The chow group is added as a black bar. Significant differences are shown with *. Plasma values are shown in panels A (Cholesterol) and B (TG). Panel C shows cholesterol concentration in each lipoprotein fraction. Panel D shows the amount of hepatic TG at the several time points with and without fibrate(dF and d). A significant difference between the group and the normal chow diet is indicated by *, and ** indicates significant difference with both the chow group and the former time point.

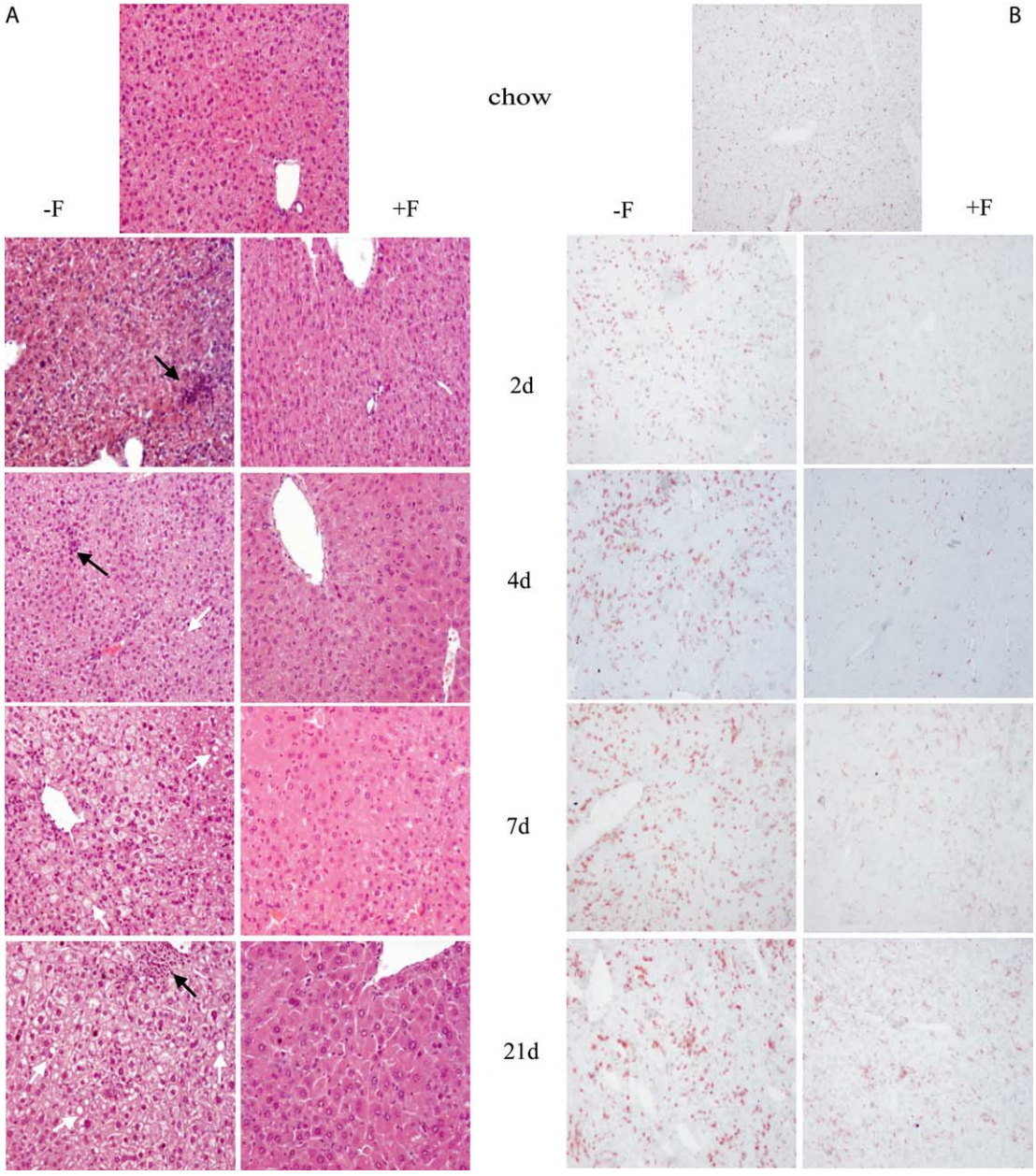

Fig. 2. Morphology of liver tissue. Panel A shows HE-stained paraffin slides. White arrows indicate fat droplets, black arrows point at inflammatory clusters. At all time points, left pictures of mice on the high-fat diet, right pictures of mice treated with fenofibrate. Panel B. Immunostaining with antibodies against CD68 and counterstained with haematoxylin. [This figure appears in colour on the web.]

Mac1 (Fig. 3). The number of Mac1-positive cells was corrected for granulocytes (also positive for Mac1), using the granulocyte-specific Nimp1 antibody. The combined data demonstrate a significant increase in the number of liver macrophages (10.3-fold) already after 2 days. At 4 days the number of macrophages further increased to a maximal level (17.8-fold). Fibrate treatment reduced the amount of macrophages substantially. Altogether, these data indicate that the increase in the number of macrophages is an early event during development of NASH and that it is prevented upon PPARα-activation.

3.4. Diet-regulated genes

Large-scale gene expression analysis showed 294 genes to be regulated; 180 (61%) showed up-regulation upon high-fat feeding, whereas 114 genes (39%) were down-regulated. We focused on genes involved in inflammation and lipid metabolism, as these two classes of genes comprised the largest groups of regulated genes (Table 1) and are directly linked to the pathological phenotype of these mice.

The increase in inflammatory genes is in line with other studies in which western diet was applied to different strains

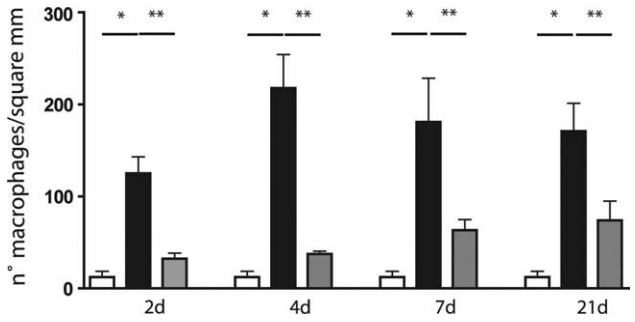

Fig. 3. Macrophages in the liver. Hepatic cryoslides were stained with antibodies against Mac1 and counted. The counting was corrected for stained granulocytes, who also express this marker. White bars indicate animals on a chow diet, black bars show data from mice fed the high-fat diet and gray bars indicate mice fed the high-fat diet supplemented with fenofibrate. Significant differences compared to the chow group are indicated by *, while ** shows significance between the fibrate-treated group and the high-fat diet-treated group. Scale expressed as cells per millimeter square.

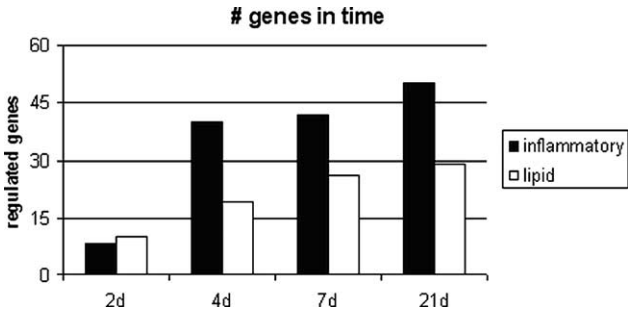

Fig. 4. Amount of lipid and inflammation genes regulated in time. This figure shows the total number of genes that are regulated by the diet at all time points. White bars indicate the lipid genes, while the black bars indicate the inflammation-related genes. Both up- and down-regulated genes are included in this figure.

of mice such as C57BL/6J and APOE3-Leiden [9,10]. Strikingly, in our model, inflammation appeared already after 2 days. Many of these inflammatory genes are regulated via the transcription factor NF-κB (i.e. vascular cell adhesion molecule 1, phospolipase A2, serum amyloid genes). Among the inflammatory genes, the acute phase response genes (i.e. serum amyloid A1, A2, A3, A4) were induced rapidly, followed by up-regulation of interferon-induced genes (i.e. interferon gamma inducible protein 30, interferon induced transmembrane protein 2, interferon-induced protein with tetratricopeptide) and heat shock proteins, indicative for the development of a stress response.

Among the lipid genes, mainly genes involved in FA biosynthesis such as stearoyl-Coenzyme A desaturase 2, lipid transport (e.g. ATP binding cassette G5 and A1; ABCG5, ABCA1) and lipid metabolism (e.g. LpL and granulin), were up-regulated.

In addition, within time the expression of collagen synthesis genes like procollagen type 1 was also up-regulated, indicating the development of fibrosis.

The number of inflammatory genes went up rapidly until day 4, indicating a quick inflammatory response in the liver. After 4 days, the increase was less pronounced. In contrast, the number of lipid genes increased steadily with time (Fig. 4). These data indicate that the early phenotypic changes in liver histology and blood parameters of APOE2KI mice fed a western diet are accompanied by massive regulation in hepatic expression of inflammatory genes followed by lipid genes.

3.5. Fibrate-regulated genes

Liver RNA from mice fed a western diet enriched with fenofibrate at two time points (2 and 7 days) was collected and hybridized to Affymetrix arrays. These time points were chosen to identify early effects, and to avoid indirect effects. Comparison to the diet-regulated genes revealed relatively small overlap, suggesting a bigger role for nuclear receptors other than PPARα in diet-induced expression (Table 1). As expected, fibrate changed the expression of many genes, including previously known PPARα responsive genes. Many of these genes are involved in processes such as lipid metabolism and inflammation. Upon fenofibrate treatment, a total of 1023 genes were regulated (compared with western diet at the corresponding time-points). Among these genes, 830 (81%) were up-regulated and 193 (19%) were down-regulated. The majority of up-regulated genes included lipid metabolism genes, such as genes involved in FA β-oxidation and lipid transport. In contrast, down-regulated genes belong to inflammatory pathways, mainly under control of NF-κB. These results are in agreement with previous studies reporting the hepatic response of other mice models to fibrate treatment [11]. In addition, the expression of procollagen synthesis genes, like procollagen type 1, was inhibited by fibrate.

3.6. Validation of the array data

The regulation of five well-known PPARα responsive genes involved in lipid metabolism (Lpl, Cte1, Cpt1, Acadvl and Acox1) was verified by QPCR. In addition, the expression of two additional genes regulated on a western diet (Ccnd1 and Fdft1) and two inflammatory genes (CD68 antigen and Nfkbia) were also determined (Table 2). To correlate the results obtained by QPCR and Affymetrix analysis of the 10 selected genes, the logarithmic values of the fold change obtained by the two techniques were compared (Fig. 5). These results indicate a significant correlation (Pearson correlation coefficient = 0.90; $P < 0.0001$).

Biological variation within each pool was checked by QPCR on individual mice for CD68 and Acox1. The degree of up and down-regulation upon treatment with western diet was found to be consistent for all individual mice (data not shown).

Collectively, the QPCR results were fully compatible with the array data and demonstrate the reliability of the microarray analysis.

Table 1
Lipid- and inflammation-related genes upon feeding a high-fat diet

Gene	2dW	4dW	7dW	21dW	2dF	7dF	Gene	2dW	4dW	7dW	21dW	2dF	7dF
Lipid metabolism genes													
Insulin induced gene 2	−1.5	ns	ns	ns	1.8	1.6	Cytochrome P450, 51	ns	ns	ns	−2.1	ns	ns
RIKEN cDNA 1600020H07 gene	ns	ns	−1.5	−1.6	ns	1.7	7-dehydrocholesterol reductase	ns	−2.1	−2.3	−2.4	ns	ns
Farnesyl diphosphate farnesyl transferase 1	ns	−2.1	−3.1	−2.4	ns	1.9	Fatty acid binding protein 5, epidermal	2.6	ns	1.7	1.5	−2.3	−2.1
3-hydroxy-3-methylglutaryl-coenzyme A synthase 1	ns	ns	−3	−4	ns	2.9	Lysosomal acid lipase 1	ns	1.4	1.4	1.5	1.6	1.4
Pancreatic lipase-related protein 2	−1.2	−2.4	−7.3	−8.4	−7	−1.2	Stearoyl-coenzyme A desaturase 1	1.2	ns	ns	ns	ns	1.9
Pancreatic lipase-related protein 1	1	−2.3	−11	−20	−23	−1.7	Fatty acid binding protein 2, intestinal	2.6	2.9	2.7	3.2	1.6	2.2
Carboxyl ester lipase	ns	ns	−9.6	−18	−21	ns	3-ketoacyl-CoA thiolase B	1.4	1.5	ns	1.5	2.4	2.8
Colipase, pancreatic	ns	ns	−14	−39	−41	ns	Lipoprotein lipase	ns	2.2	2.8	4.2	2.2	3.3
Isopentenyl-diphosphate delta isomerase	ns	−4.2	−4.2	−5.2	−3.3	ns	Granulin	ns	1.4	ns	1.6	1.5	ns
Sterol-C4-methyl oxidase-like	ns	−3.6	−3.9	−3.6	−2.5	ns	ATP-binding cassette, sub-family G, 5	ns	1.7	1.5	2	1.7	ns
Acetyl-CoA synthetase 2 (ADP forming)	−1.8	−2.3	−3.2	−3.3	−2.7	ns	Prosaposin	ns	1.8	1.8	1.9	1.6	ns
NAD(P) dependent steroid dehydrogenase-like	ns	−2.1	−2.1	−2.4	−2.2	ns	ATP-binding cassette, sub-family A, 1	ns	1.9	1.9	2.1	ns	ns
Phospholipase A2, group IB, pancreas	ns	ns	−2.9	−3	ns	ns	Stearoyl-coenzyme A desaturase 2	ns	2.8	2.6	3	ns	ns
Sterol-C5-desaturase homolog (*S. cerevisae*)	−1.4	−1.4	−1.5	−1.5	ns	ns	Fatty acid binding protein 7, brain	ns	2.8	ns	ns	ns	ns
Sulfotransferase, hydroxysteroid preferring 2	ns	ns	−2.4	−2.6	ns	ns	Phospholipid transfer protein	ns	ns	ns	2	ns	ns
Phenylalkylamine Ca2+ antagonist binding protein	ns	ns	−1.6	ns	ns	ns	Apolipoprotein B	1.3	ns	ns	ns	ns	ns
NADH dehydrogenase1,alpha/beta 1	ns	ns	−1.6	ns	ns	ns	Lipopolysaccharide binding protein	1.6	1.7	1.6	1.6	ns	ns
Fatty acid synthase	ns	ns	ns	−1.5	ns	ns	Apolipoprotein A-IV	3.9	3.9	4.2	4.1	ns	ns
Inflammatory genes													
C-type lectin, superfamily member 13	ns	1.8	1.9	1.6	ns	−1.5	Immunoglobulin heavy chain 6, IgM	ns	1.7	ns	ns	ns	ns
Interferon-induced protein with tetratricopeptide repeats 1	3	ns	ns	ns	−2.5	ns	Interferon induced transmembrane protein 2	ns	1.6	1.4	1.3	ns	ns
Orosomucoid 2	ns	3.4	3.9	ns	ns	−6.2	Catenin beta	ns	ns	ns	1.5	ns	ns
Serum amyloid A 1	6.1	7.3	9.8	5.8	−9.8	−26	CD44 antigen	ns	2.8	2.4	2.6	ns	ns
Serum amyloid A 2	5.2	5.8	9	4.9	−7.3	−17	CD52 antigen	ns	2.5	2.5	2.9	ns	ns
Serum amyloid A 3	ns	5.6	6	3.8	−2.4	−6.5	CD68 antigen	ns	3.7	3.7	4	ns	ns
Serum amyloid A 4	2	1.9	1.7	ns	−2.7	−2.7	cDNA sequence BC032204	ns	2.3	ns	2.6	ns	ns
T-cell specific GTPase	3	ns	ns	ns	−4.2	ns	Chemokine (C–C motif) ligand 6	ns	3.5	3.7	4.1	ns	ns
Regenerating islet-derived 2	−4.9	−10	−11	−12	−1.2	ns	Complement component 1, q alpha polypeptide	ns	1.7	1.8	2	ns	ns
Regenerating islet-derived 1	ns	−3.1	−19	−36	−2.3	ns	Complement component 1, q beta polypeptide	ns	2.3	2.2	2.8	ns	ns
Phospholipase A2, group IB, pancreas	ns	ns	−2.9	−3	−2.7	ns	Complement component 1, q gamma polypeptide	ns	2.3	2.4	2.9	ns	ns
Early growth response 1	−3.3	−2.1	−2.4	−2.3	2.6	ns	C-type lectin, superfamily member 12	ns	3.7	4.3	5.2	ns	ns

Table 1 (*continued*)

Gene	2dW	4dW	7dW	21dW	2dF	7dF	Gene	2dW	4dW	7dW	21dW	2dF	7dF
Heat shock protein 1, alpha	ns	1.8	1.7	1.9	3.1	2.1	C-type lectin, superfamily member 10	Ns	ns	ns	2.3	ns	ns
Heat shock protein 105	ns	1.7	ns	ns	1.9	ns	Immunoglobulin kappa chain variable 28 (V28)	ns	2.8	ns	2.4	ns	ns
Heat shock protein 1B	ns	ns	3.2	3.3	5	ns	Interferon activated gene 203	Ns	2.1	2	2.3	ns	ns
Lectin, galactose binding, soluble 1	ns	ns	1.7	1.7	1.6	2	Interferon gamma inducible protein 30	ns	2.5	2.5	2.5	ns	ns
Phospholipase A2, group VII	ns	ns	2	2.6	ns	2.4	Lymphocyte antigen 86	ns	2.1	2.1	2.2	ns	ns
S100 calcium binding protein A8	2.1	2.9	2.3	3.3	1.5	ns	Macrophage receptor with collagenous structure	ns	2.2	2.6	2	ns	ns
C-type lectin-like receptor 2	ns	2.8	2.4	2.9	ns	ns	Matrix metalloproteinase 12	ns	ns	3	4.2	ns	ns
Cytotoxic T lymphocyte-associated protein 2b	ns	2.4	ns	ns	ns	ns	Procollagen, type I, alpha 1	ns	ns	2.4	2.5	ns	ns
Eosinophil-associated, ribonuclease A 2 family	ns	2	2.3	2.9	ns	ns	Procollagen, type III, alpha 1	ns	2.8	3.7	4.3	ns	ns
Glycoprotein (transmembrane) nmb	ns	ns	2.8	5.2	ns	ns	Procollagen, type IV, alpha 1	ns	1.8	2.1	2.2	ns	ns
Heat shock protein 8	ns	ns	ns	1.5	ns	ns	Procollagen, type XIV, alpha 1	ns	ns	ns	1.6	ns	ns
Histocompatibility 2, class II antigen A, alpha	ns	ns	2.3	2.9	ns	ns	Protein tyrosine phosphatase, non-receptor type substrate 1	ns	2.6	2.7	3.2	ns	ns
Histocompatibility 2, class II antigen A, beta 1	ns	ns	ns	2.8	ns	ns	Transforming growth factor, beta induced	ns	1.6	ns	1.8	ns	ns
Histocompatibility 2, class II antigen E beta	ns	ns	1.9	2.3	ns	ns	Vascular cell adhesion molecule 1	ns	2.6	2.3	2.3	ns	ns
							Pancreatitis-associated protein	ns	−2.9	−2.8	−3.3	ns	ns

Genes in this table are all regulated by only diet or by diet and fibrate treatment. Fold changes of gene expression of the animals fed the high-fat diet are shown relative to gene expression in the chow-fed group. Fold changes of the gene expression of the fibrate-treated animals is shown relative to the high-fat treated animals at the same time point.

4. Discussion

In the present study, we show that APOE2KI mice develop NASH in response to western diet, which can be inhibited by fibrate treatment.

To our knowledge, in all other studies performed with the APOE2KI mice, liver morphology was not subject of investigation [3,12–14]. Interestingly, already within 4 days of high-fat feeding these mice develop a marked liver phenotype characterised by steatosis, inflammation and early fibrosis. The reason for this rapid response is not yet clear. It has been suggested that the ApoE protein, in addition to its role in lipoprotein clearance, has a physiological function in the VLDL assembly-secretion cascade [15]. Thus, it is feasible that the balance between FA uptake and secretion is affected in the APOE2KI mouse due to impaired VLDL secretion. Alternatively, it is possible that the free FA synthesis and esterification or uptake is increased. In addition, it has been shown that ApoE can have a direct effect on tissue macrophage recruitment, independent of lipoprotein metabolism [16,17]. Thus, the APOE2KI mice may be highly sensitive to develop inflammation regardless of the steatosis. Other hyperlipidemic mouse models, such as ldlr$^{-/-}$ mice and apoe$^{-/-}$ mice also develop a similar phenotype upon long periods of high-fat feeding [18,19]. Moreover, C57BL6 mice, fed an atherogenic diet for 4–5 weeks, were also shown to induce hepatic lipid and inflammatory genes [9,20] and to develop this phenotype [18].

It has been shown that MCD (methionine and choline deficient) diet-induced fibrosing steatohepatitis in mice can be reversed by treatment with Wy-14,643, a PPARalpha agonist [21]. In our study, fibrate administration prevents the accumulation of hepatic triglycerides, which is consistent with the up-regulation of a large number of genes involved in peroxisomal and mitochondrial β-oxidation. In addition, it prevents the infiltration of macrophages into the liver, consistent with the regulation of anti-inflammatory genes.

The high percentage of saturated FAs in the diet (21% butter) is most likely to be responsible for the acute inflammatory response [22–24]. Vergnes et al. [25] have shown that cholesterol is also contributing to the induction

Table 2
Primer sequences for real-time quantitative PCR analysis

Gene symbol	Gene name	Probeset ID affymetrix	Forward primer	Reversed primer
Lpl	Lipoprotein lipase	1415904_at	5′-GAT GCC CTA CAA AGT GTT CCA-3′	5′-GCC ACT GTG CCG TAC AGA GA-3′
Cte1	Cytosolic acyl-CoA thioesterase 1	1449065_at	5′-GCA GCC ACC CCG AGG TAA A-3′	5′-GCC ACG GAG CCA TTG ATG-3′
Fdft1	Farnesyl diphosphate farnesyl transferase 1	1448130_at	5′-CCC TGA CGT CCT CAC CTA CCT-3′	5′-GGC CAT TAC CTG TGG AAT AGC A-3′
Acadvl	Acyl-coenzyme A dehydrogenase very long chain	1424184_at	5′-AGA CGG AGG ACA GGA ATC GG-3′	5′-ACC ACG GTG GCA AAT TGA TC-3′
Acox1	Acyl-CoA Oxidase 1, peroxisomal	1416408_at	5′-CTT GAG GGG AAC ATC ATC ACA-3′	5′-GCC AAG GGT CAC ATC CTT AAA GT-3′
Ccnd1	Cyclin D1	1448698_at	5′-TAC CGC ACA ACG CAC TTT CTT-3′	5′-CGC AGG CTT GAC TCC AGA AG-3′
Cpt1a	Carnitine palmitoyltransferase 1a, liver	1460409_at	5′-ACC CCA CAA CAA CGG CAG A-3′	5′-GCC AGC GCC CGT CAT-3′
CD68	CD68 antigen	1449164_at	5′-TGA CCT GCT CTC TCT AAG GCT ACA-3′	5′-TCA CGG TTG CAA GAG AAA CAT G-3′
Nfkbia (Ikb alpha)	Nuclear factor of kappa light chain gene	1448306_at	5′-TGG AAG TCA TTG GTC AGG TGA A-3′	5′-CAG AAG TGC CTC AGC AAT TCC T-3′
Cyclophilin A	Cyclosporin A-binding protein	1417451_a_at	5′-CAA ATG CTG GAC CAA ACA CAA-3′	5′-GCC ATC CAG CCA TTC AGT CT-3′

of genes involved in acute inflammation, including genes of the serum amyloid A family and various cytokine-related genes.

Comparison between genes regulated by diet and genes regulated by addition of fenofibrate to the diet revealed relatively small overlap. Some of the established PPARα regulated genes (e.g. Acox1, Cte1) were not regulated when mice were fed a western diet. Possibly many of the diet-regulated genes were not detected due to a low level of difference in regulation compared with chow.

Other transcription factors play a more prominent role in regulation of lipid genes by the diet. Indeed, changes in lipid genes (e.g. sterol-C4-methyl oxidase-like, sterol-C5-desaturase and FA synthase) are attributable to SREBP-activation [26]. Similarly, several LXR-responsive genes were regulated such as ATP-binding cassette, sub-family A1, stearoyl-coenzyme A desaturase 1 and FA binding protein.

Among the inflammatory genes regulated upon western diet, several genes contained functional NF-κB binding sites in their promoter regions. NF-κB plays a crucial role in inflammation, by regulating the production of various cytokines that can trigger several inflammatory reactions [27]. Conversely, NF-κB cascade induces alterations in FA metabolism [28].

The massive repression of inflammatory gene-expression might be related to the ability of PPARα to interfere with the NF-κB pathway [29,30]. The early down-regulation in the expression of inflammatory genes suggests that the prevention of steatohepatitis by fibrates may be a direct consequence of their anti-inflammatory effect.

Strikingly, in this mouse model the increase in macrophages in the liver preceded the accumulation of fat. The function of these macrophages in the pathogenesis of steatosis as observed in these mice is not yet clear. Similarly, the reduction in the expression of inflammatory genes occurred immediately after fibrate treatment, suggesting that inflammation may play an instrumental role during the development of NASH. These data are in contradiction with the current mechanistic concept of the disease in which an initial metabolic disturbance causes steatosis and a second pathogenic event leads to inflammation [31]. In support of our observation, it has been

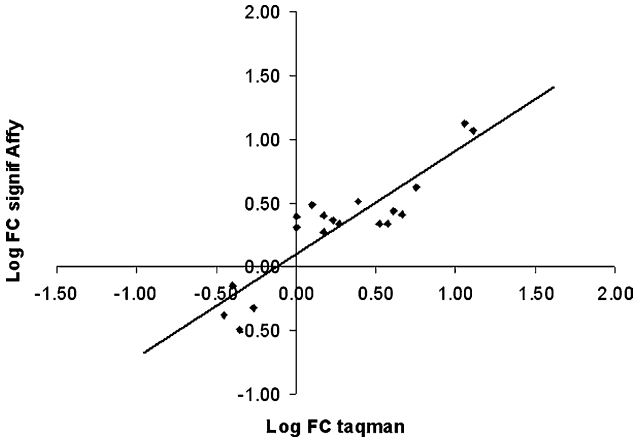

Fig. 5. Verification of chip data with QPCR. Graph showing log values of fold changes of both QPCR and microarray data. When plotted, a clear correlation can be seen with a Pearsson correlation coefficient of 0.8971 and $P < 0.0001$.

shown that inflammation, possibly mediated via NF-κB-regulated cytokines, can influence lipid metabolism. Plasma VLDL levels were found to increase due to enhanced adipose tissue lipolysis, increased de novo hepatic FA synthesis and suppression of FA oxidation [32,33]. Changes in lipid metabolism during the acute phase response have been attributed to decreases in the levels of several nuclear hormone receptors, including PPARα. Pharmacological activation of PPARα in C57BL6 mice fed the MCD diet resulted in a marked attenuation of the NASH phenotype, affecting both steatosis and inflammation [21,34]. The collective findings suggest that the observed effects are not dependent on the specific model used.

At present, there is no effective treatment for NASH [35] and therefore further studies exploring the role of macrophages in early stages of NASH, can contribute to the design of effective therapeutic strategies for treatment and prevention of NASH.

Acknowledgements

We are grateful to Prof. Wim Buurman, Prof. Wout Lamers and Prof. Ger van der Vusse for helpful discussions. We thank Monique Vergouwe, Inge van der Made and Mathijs Groeneweg for technical support. This research is supported by The Netherlands Hart Foundation (NHS) (grant 2002B018) and by the NIH, grant HL42630.M. van Bilsen is an Established Investigator of The Netherlands Heart Foundation. Bart Staels and Marten H. Hofker are part of the European Vascular genomics network (EVGN).

References

[1] Ludwig J, Viggiano TR, McGill DB, Oh BJ. Nonalcoholic steatohepatitis: Mayo Clinic experiences with a hitherto unnamed disease. Mayo Clin Proc 1980;55:434–438.
[2] Ludwig J, McGill DB, Lindor KD. Review: nonalcoholic steatohepatitis. J Gastroenterol Hepatol 1997;12:398–403.
[3] Sullivan PM, Mezdour H, Quarfordt SH, Maeda N. Type III hyperlipoproteinemia and spontaneous atherosclerosis in mice resulting from gene replacement of mouse Apoe with human Apoe*2. J Clin Invest 1998;102:130–135.
[4] Duval C, Fruchart JC, Staels B. PPAR alpha, fibrates, lipid metabolism and inflammation. Arch Mal Coeur Vaiss 2004;97:665–672.
[5] Zambon A, Hashimoto SI, Brunzell JD. Analysis of techniques to obtain plasma for measurement of levels of free fatty acids. J Lipid Res 1993;34:1021–1028.
[6] Ghesquiere SA, Gijbels MJ, Anthonsen M, van Gorp PJ, van der Made I, Johansen B, et al. Macrophage-specific overexpression of group IIa sPLA2 increases atherosclerosis and enhances collagen deposition. J Lipid Res 2005;46:201–210.
[7] Pelsers MM, Butler PJ, Bishop CM, Glatz JF. Fatty acid binding protein in heart and skeletal muscles of the migratory barnacle goose throughout development. Am J Physiol 1999;276:R637–R643.
[8] Hoogwerf BJ, Bantle JP, Kuba K, Frantz Jr ID, Hunninghake DB. Treatment of type III hyperlipoproteinemia with four different treatment regimens. Atherosclerosis 1984;51:251–259.
[9] Kim S, Sohn I, Ahn JI, Lee KH, Lee YS. Hepatic gene expression profiles in a long-term high-fat diet-induced obesity mouse model. Gene 2004;340:99–109.
[10] Kreeft AJ, Moen CJ, Hofker MH, Frants RR, Vreugdenhil E, Gijbels MJ, et al. Identification of differentially regulated genes in mildly hyperlipidemic ApoE3-Leiden mice by use of serial analysis of gene expression. Arterioscler Thromb Vasc Biol 2001;21:1984–1990.
[11] Yamazaki K, Kuromitsu J, Tanaka I. Microarray analysis of gene expression changes in mouse liver induced by peroxisome proliferator-activated receptor alpha agonists. Biochem Biophys Res Commun 2002;290:1114–1122.
[12] Knouff C, Malloy S, Wilder J, Altenburg MK, Maeda N. Doubling expression of the low density lipoprotein receptor by truncation of the 3′-untranslated region sequence ameliorates type iii hyperlipoproteinemia in mice expressing the human apoe2 isoform. J Biol Chem 2001;276:3856–3862.
[13] Hinsdale ME, Sullivan PM, Mezdour H, Maeda N. ApoB-48 and apoB-100 differentially influence the expression of type-III hyperlipoproteinemia in APOE*2 mice. J Lipid Res 2002;43:1520–1528.
[14] Knouff C, Briand O, Lestavel S, Clavey V, Altenburg M, Maeda N. Defective VLDL metabolism and severe atherosclerosis in mice expressing human apolipoprotein E isoforms but lacking the LDL receptor. Biochim Biophys Acta 2004;1684:8–17.
[15] Kuipers F, Jong MC, Lin Y, Eck M, Havinga R, Bloks V, et al. Impaired secretion of very low density lipoprotein–triglycerides by apolipoprotein E-deficient mouse hepatocytes. J Clin Invest 1997;100:2915–2922.
[16] Lessner SM, Prado HL, Waller EK, Galis ZS. Atherosclerotic lesions grow through recruitment and proliferation of circulating monocytes in a murine model. Am J Pathol 2002;160:2145–2155.
[17] Grainger DJ, Reckless J, McKilligin E. Apolipoprotein E modulates clearance of apoptotic bodies in vitro and in vivo, resulting in a systemic proinflammatory state in apolipoprotein E-deficient mice. J Immunol 2004;173:6366–6375.
[18] Yoshimatsu M, Terasaki Y, Sakashita N, Kiyota E, Sato H, van der Laan LJ, et al. Induction of macrophage scavenger receptor MARCO in nonalcoholic steatohepatitis indicates possible involvement of endotoxin in its pathogenic process. Int J Exp Pathol 2004;85:335–343.
[19] Tous M, Ferre N, Camps J, Riu F, Joven J. Feeding apolipoprotein E-knockout mice with cholesterol and fat enriched diets may be a model of non-alcoholic steatohepatitis. Mol Cell Biochem 2005;268:53–58.
[20] Liao F, Andalibi A, deBeer FC, Fogelman AM, Lusis AJ. Genetic control of inflammatory gene induction and NF-kappa B-like transcription factor activation in response to an atherogenic diet in mice. J Clin Invest 1993;91:2572–2579.
[21] Ip E, Farrell G, Hall P, Robertson G, Leclercq I. Administration of the potent PPARalpha agonist, Wy-14,643, reverses nutritional fibrosis and steatohepatitis in mice. Hepatology 2004;39:1286–1296.
[22] Tripathy D, Mohanty P, Dhindsa S, Syed T, Ghanim H, Aljada A, et al. Elevation of free fatty acids induces inflammation and impairs vascular reactivity in healthy subjects. Diabetes 2003;52:2882–2887.
[23] Doshi M, Watanabe S, Niimoto T, Kawashima H, Ishikura Y, Kiso Y, et al. Effect of dietary enrichment with n-3 polyunsaturated fatty acids (PUFA) or n-9 PUFA on arachidonate metabolism in vivo and experimentally induced inflammation in mice. Biol Pharm Bull 2004;27:319–323.
[24] Calder PC. Fatty acids and gene expression related to inflammation. Nestle Nutr Workshop Ser Clin Perform Programme 2002;7:19–36 [discussion 36–40].

[25] Vergnes L, Phan J, Strauss M, Tafuri S, Reue K. Cholesterol and cholate components of an atherogenic diet induce distinct stages of hepatic inflammatory gene expression. J Biol Chem 2003;278: 42774–42784.
[26] Horton JD, Shah NA, Warrington JA, Anderson NN, Park SW, Brown MS, et al. Combined analysis of oligonucleotide microarray data from transgenic and knockout mice identifies direct SREBP target genes. Proc Natl Acad Sci USA 2003;100:12027–12032.
[27] Collins T, Cybulsky MI. NF-kappaB: pivotal mediator or innocent bystander in atherogenesis? J Clin Invest 2001;107:255–264.
[28] Feingold KR, Soued M, Serio MK, Moser AH, Dinarello CA, Grunfeld C. Multiple cytokines stimulate hepatic lipid synthesis in vivo. Endocrinology 1989;125:267–274.
[29] Delerive P, De Bosscher K, Besnard S, Vanden Berghe W, Peters JM, Gonzalez FJ, et al. Peroxisome proliferator-activated receptor alpha negatively regulates the vascular inflammatory gene response by negative cross-talk with transcription factors NF-kappaB and AP-1. J Biol Chem 1999;274:32048–32054.
[30] Delerive P, Gervois P, Fruchart JC, Staels B. Induction of IkappaBalpha expression as a mechanism contributing to the anti-inflammatory activities of peroxisome proliferator-activated receptor-alpha activators. J Biol Chem 2000;275:36703–36707.
[31] Day CP, James OF. Steatohepatitis: a tale of two 'hits'? Gastroenterology 1998;114:842–845.
[32] Feingold KR, Soued M, Serio MK, Adi S, Moser AH, Grunfeld C. The effect of diet on tumor necrosis factor stimulation of hepatic lipogenesis. Metabolism 1990;39:623–632.
[33] Khovidhunkit W, Kim MS, Memon RA, Shigenaga JK, Moser AH, Feingold KR, et al. Effects of infection and inflammation on lipid and lipoprotein metabolism: mechanisms and consequences to the host. J Lipid Res 2004;45:1169–1196.
[34] Ip E, Farrell GC, Robertson G, Hall P, Kirsch R, Leclercq I. Central role of PPARalpha-dependent hepatic lipid turnover in dietary steatohepatitis in mice. Hepatology 2003;38:123–132.
[35] Liangpunsakul S, Chalasani N. Treatment of nonalcoholic fatty liver disease. Curr Treat Options Gastroenterol 2003;6:455–463.